

Ab initio Approach to Collective Excitations in Excitonic Insulators

Fengyuan Xuan,^{1,*} Jiexi Song,¹ and Zhiyuan Sun^{2,3,†}

¹Suzhou Laboratory, Suzhou, 215123, China

²State Key Laboratory of Low-Dimensional Quantum Physics and Department of Physics, Tsinghua University, Beijing 100084, P. R. China

³Frontier Science Center for Quantum Information, Beijing 100084, P. R. China

(Dated: December 25, 2025)

An *ab initio* approach is presented for studying the collective excitations in excitonic insulators, charge/spin density waves and superconductors. We derive the Bethe-Salpeter-Equation for the particle-hole excitations in the quasiparticle representation, from which the collective excited states are solved and the corresponding order parameter fluctuations are computed. This method is demonstrated numerically for the excitonic insulating phases of the biased WSe₂-MoSe₂ bilayer. It reveals the gapless phase-mode, the subgap Bardasis-Schrieffer modes and the above-gap scattering states. Our work paves the way for quantitative predictions of excited state phenomena from first-principles calculations in electronic systems with spontaneous symmetry breaking.

Ab initio approaches based on density functional theory (DFT) combined with many-body perturbation theory (MBPT) [1] are widely used to study many-electron systems. For systems with spontaneous symmetry breaking such as superconductors and excitonic insulators, first-principles methods for their ground states have been established [2–8]. However, their collective excitations [9, 10] are still inaccessible within the *ab initio* framework.

The excitonic insulator (EI), proposed six decades ago [11, 12], has seen a revival in recent years [13]. It refers to a long range ordered state formed by bounded electron-hole (*e-h*) pairs which spontaneously breaks either the *U*(1) symmetry of exciton number conservation or discrete lattice symmetries [13–19]. Recent experiments vibrantly searched for EI states in bulk materials such as Ta₂NiSe₅ [20–28], WTe₂ [29, 30] and Ta₂Pd₃Te₅ [31], and established stable exciton fluids in *e-h* bilayer systems [32–37]. The collective excitations of the condensate correspond to fluctuations of the order parameter [17, 19, 38–42], which govern optical responses and may serve as their experimental signatures. Analytical approaches to these modes rely on model Hamiltonians [19, 39, 40, 42–46], whereas realistic material calculations call for a computational formalism natively compatible with first-principles packages.

In this work, we present an *ab initio* approach for quantitative computation of collective excitations using the Bethe-Salpeter-Equation (BSE) for typical systems with spontaneously broken symmetry. While the presented formula apply equally well to generic systems such as superconductors and charge/spin density waves, we focus our discussion on EIs. On top of the mean field Hamiltonian, we construct from the fluctuation terms the BSE eigenvector/eigenvalue equation for particle-hole pair excitations. The eigenvectors and eigenvalues are those for collective excited states, from which the excitonic order parameter fluctuations are also computed. We demonstrate our method in the biased WSe₂-MoSe₂ system and reveal the zero-energy phase-mode and a series of subgap Bardasis-Schrieffer (BaSh) modes [10, 39, 42].

We start from the Hamiltonian that includes multiple conduction and valence bands [11, 12, 47, 48]:

$$H = \sum_{ck} \xi_{ck} c_{ck}^\dagger c_{ck} + \sum_{vk} \xi_{vk} c_{vk}^\dagger c_{vk} - \sum_{vck, v'c'k'} V_{vck, v'c'k'} c_{c'k'}^\dagger c_{v'k'} c_{vk}^\dagger c_{ck} \quad (1)$$

where ξ_{nk} is the single particle energy, c (v) is an integer that runs over all conduction (valence) bands, and $V_{vck, v'c'k'}$ consists of the direct and exchange *e-h* interactions. These parameters are obtained from standard first-principles DFT and MBPT calculations [49–51]. For notational simplicity, the other two-body interaction terms such as electron-electron (*e-e*) and hole-hole (*h-h*) interactions are neglected and will be discussed later. The *e-h* pairing terms with non-zero center-of-mass momenta are not shown explicitly because we focus on zero momentum condensate and excitations in this paper. As shown by Eq. (1), we limit our calculation to the case of conserved exciton number so that the possible EI state breaks the continuous *U*(1) symmetry. The effects of intrinsic interband tunneling [14, 18, 19, 43] and electron-phonon coupling [13, 15–17] will be addressed in future works.

We separate the Hamiltonian into mean-field (MF) and fluctuation parts: $H = H_{\text{MF}} + H_{\text{fluc}}$ [52–54]. The MF Hamiltonian reads

$$H_{\text{MF}} = H_0 + \sum_{ck} E_{ck} \gamma_{ck}^\dagger \gamma_{ck} + \sum_{vk} E_{vk} \gamma_{vk}^\dagger \gamma_{vk}, \quad (2)$$

which is obtained from diagonalizing

$$h_k = \begin{bmatrix} \dots & \dots & \dots & \dots & \dots & \dots & \dots \\ \dots & \xi_{c_2 k} & 0 & -\Delta_{v_1 c_2 k} & -\Delta_{v_2 c_2 k} & \dots & \dots \\ \dots & 0 & \xi_{c_1 k} & -\Delta_{v_1 c_1 k} & -\Delta_{v_2 c_1 k} & \dots & \dots \\ \dots & -\Delta_{v_1 c_2 k}^* & -\Delta_{v_1 c_1 k}^* & \xi_{v_1 k} & 0 & \dots & \dots \\ \dots & -\Delta_{v_2 c_2 k}^* & -\Delta_{v_2 c_1 k}^* & 0 & \xi_{v_2 k} & \dots & \dots \\ \dots & \dots & \dots & \dots & \dots & \dots & \dots \end{bmatrix} \quad (3)$$

by the unitary matrix U , $U^\dagger h_k U = \text{diag}(E_{nk})$. Here Δ_{vck} is the band and momentum dependent excitonic order parameter. The annihilation operators γ_{ck} (γ_{vk}) are for the quasiparticles in the conduction (valence) bands with quasiparticle energies E_{ck} (E_{vk}) renormalized by excitonic order. They

* Contact author: xuanfy@szlab.ac.cn

† Contact author: zysun@tsinghua.edu.cn

are related to the bare electronic annihilation operators as $c_{nk} = \sum_m U_{nk}^{mk} \gamma_{mk}$. The MF ground state is that of the MF Hamiltonian Eq. (2), and could be written as $|\text{MF}\rangle = \prod_{vk} (U_{vk}^{vk} + \sum_c U_{ck}^{vk} c_{ck}^\dagger c_{vk}) |\text{HF}\rangle$ if the normal state $|\text{HF}\rangle$ is a semiconductor. The gap equation at zero temperature reads

$$\Delta_{vck} = \sum_{v'c'k'} V_{v'c'k', vck} \varphi_{v'c'k'}, \quad (4)$$

where $\varphi_{vck} \equiv \langle c_{vk}^\dagger c_{ck} \rangle = \sum_{v_0} U_{vk}^{v_0 k*} U_{ck}^{v_0 k}$. In the Bose-

Einstein Condensation (BEC) limit where the exciton size is much smaller than the inter-exciton distance, φ_{vck} may be interpreted as the excitonic wave function. From Eq. (3) and Eq. (S9), the quasiparticle energies, U -matrix and EI state can be calculated self-consistently.

We now present the BSE for the collective excitations. The fluctuation Hamiltonian is $H_{\text{fluc}} = - \sum_{vck, v'c'k'} V_{vck, v'c'k'} (c_{c'k'}^\dagger c_{v'k'} - \varphi_{v'c'k'}^*) (c_{vk}^\dagger c_{ck} - \varphi_{vck})$ which in the quasi-particle basis reads

$$H_{\text{fluc}} = - \sum_{vck, v'c'k'} V_{vck, v'c'k'} \left(\sum_{n'm'} U_{c'k'}^{m'k'*} U_{v'k'}^{n'k'} \gamma_{m'k'}^\dagger \gamma_{n'k'} - \varphi_{v'c'k'}^* \right) \left(\sum_{nm} U_{vk}^{nk*} U_{ck}^{mk} \gamma_{nk}^\dagger \gamma_{mk} - \varphi_{vck} \right), \quad (5)$$

With the interaction term H_{fluc} turned on, the ground state is modified from $|\text{MF}\rangle$ to the true ground state $|0\rangle$ which is a linear combination of $|\text{MF}\rangle$ and states with multi quasi e - h pairs. The (one pair) collective excited states on top of the true ground state may be written as

$$|S\rangle = \sum_{vck} (A_{vck}^{S*} \gamma_{ck}^\dagger \gamma_{vk} - B_{vck}^{S*} \gamma_{vk}^\dagger \gamma_{ck}) |0\rangle \quad (6)$$

$$\begin{aligned} \Pi_{vck, v'c'k'}^{AA} &= - \sum_{v_1 c_1, v'_1 c'_1} \left(V_{v_1 c_1 k, v'_1 c'_1 k'} U_{c'_1 k'}^{c'k'*} U_{v'_1 k'}^{v'k'} U_{v_1 k}^{vk*} U_{c_1 k}^{ck} + V_{v'_1 c'_1 k', v_1 c_1 k} U_{c_1 k}^{vk*} U_{v_1 k}^{ck} U_{v'_1 k'}^{c'k'*} U_{c'_1 k'}^{v'k'} \right), \\ \Pi_{vck, v'c'k'}^{AB} &= - \sum_{v_1 c_1, v'_1 c'_1} \left(V_{v_1 c_1 k, v'_1 c'_1 k'} U_{c_1 k}^{ck} U_{v_1 k}^{vk*} U_{v'_1 k'}^{c'k'*} U_{c'_1 k'}^{v'k'*} + V_{v'_1 c'_1 k', v_1 c_1 k} U_{c'_1 k'}^{c'k'*} U_{v'_1 k'}^{v'k'*} U_{v_1 k}^{ck} U_{c_1 k}^{vk*} \right). \end{aligned} \quad (8)$$

Because the BSE matrix is self-adjoint with respect to $\sigma_3 = \text{diag}(\hat{I}, -\hat{I})$ in the A, B space, the eigen vectors $X_S = (A^S, B^S)^T$ could be made orthonormal to each other with the properly defined inner product: $X_S^\dagger \sigma_3 X_{S'} = \delta_{SS'}$. One may also view Eq. (7) as the eigen equation for determining the canonical bosonic operators $a_S^\dagger = \sum_{vck} (A_{vck}^{S*} \gamma_{ck}^\dagger \gamma_{vk} - B_{vck}^{S*} \gamma_{vk}^\dagger \gamma_{ck})$ for collective modes, see Appendix A. The normalization condition is simply the requirement of the bosonic commutation relation: $[a_S, a_{S'}^\dagger] = \delta_{SS'}$. The eigen energies Ω_S , coming in positive-negative pairs, are equivalent to those from the Green's function method [39, 40, 42]. In the limit of a normal semiconductor with zero excitonic order parameter, the U -matrix is identity and Eq. (7) reduces to the usual Tamm-Dancoff Approximation (TDA) of BSE for excitons.

These excited states may be viewed as the first excited states of the bosonic modes corresponding to order parameter fluctuations [9, 10, 39]. Its profile $\delta\Delta_{vck}$ may be defined

labeled by the integer S . From the equations-of-motion (EOM) method [55, 56], one obtains the BSE for the excited states in the matrix form (Appendix A):

$$\begin{bmatrix} K + \Pi^{AA} & \Pi^{AB} \\ -\Pi^{AB*} & -K - \Pi^{AA*} \end{bmatrix} \begin{bmatrix} A^S \\ B^S \end{bmatrix} = \Omega_S \begin{bmatrix} A^S \\ B^S \end{bmatrix}, \quad (7)$$

where Ω_S is the excitation energy and $K_{vck, v'c'k'} = (E_{ck} - E_{vk}) \delta_{vck, v'c'k'}$ is the kinetic energy of free quasi e - h pair. The BSE scattering kernels are

as [52]:

$$\delta\Delta_{vck} = \langle 0 | \sum_{v'c'k'} V_{v'c'k', vck} c_{v'k'}^\dagger c_{c'k'} | S \rangle + (S \leftrightarrow 0). \quad (9)$$

The neglected two-body interactions such as e - e and h - h interactions can be treated with the standard MF approach in the same manner. Their MF terms should be added to Eq. (3) and their fluctuation terms give extra contributions to the BSE kernel in Eq. (8) [52]. We also note that in Eq. (1), the interaction matrix elements are those screened by high energy degrees of freedom not included in the model. However, for the calculation of excitons and excitonic orders, one may also include the screening effect from the degrees of freedom in Eq. (1) itself [57], which may be rationalized by integrating out the degrees of freedom at energies higher than the excitonic order one cares about. In practice, because the excitonic condensation leads to change of the dielectric function compared to the normal state, the gap equation and the dielectric screening of the interaction should be solved self-consistently.

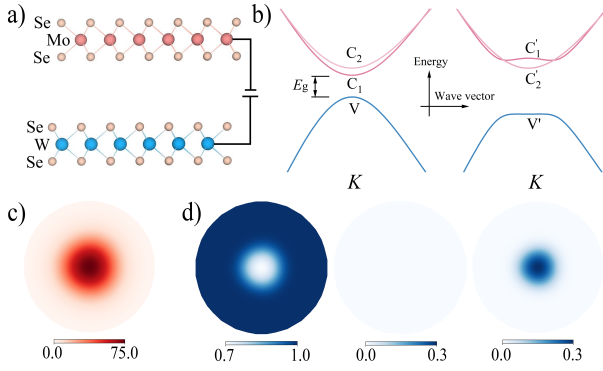


FIG. 1. (a) Atomic structure of the biased WSe₂-MoSe₂ bilayer. (b) Band structure of the normal state (left) and the EI state in the BEC regime (right) where $E_g = E_b/2$. (c) Plot of the order parameter $|\Delta_{vc1k}|$ (meV) in momentum space. (d) Plot of the U -matrix elements: $|U_{vvk}|^2$, $|U_{vc2k}|^2$ and $|U_{vc1k}|^2$ from left to right.

With Eqs. 1-9, we have described the general formalism suitable for first-principles calculation of the collective excitations in EIs without resorting to the Green's function technique. Next, we implement this method in existing software packages [49–51] and present results for the prototypical system, the biased WSe₂-MoSe₂ structure which is promising for realizing exciton condensation [32–36, 58].

As shown in Fig. 1(a), a vacuum layer equal to the thickness of monolayer hexagonal Boron Nitride (hBN) is inserted in between the *AB*-stacked WSe₂-MoSe₂ so that interlayer tunneling is neglected. For simplicity, we neglect dielectric screening from the environment including hBN but include that from the WSe₂-MoSe₂ bilayer itself [59, 60]. With no bias/gate voltage applied, the system is a semiconductor of type-II band alignment with the valence/conduction band residing on the WSe₂/MoSe₂ layer, respectively, and the *GW* band gap is $E_g \approx 2.0$ eV. The binding energy of interlayer excitons is calculated to be $E_b \approx 130$ meV, not enough to overcome the band gap. To reduce the band gap, one may apply an out-of-plane electric field using a gate voltage, or more practically, apply a chemical potential bias μ using electrical contacts shown in Fig. 1(a). The effect of the latter is equivalently modeled as a shift of the conduction band ($\xi_{ck} = \epsilon_{ck} - \mu$) on the MoSe₂ layer in Eq. (1) so that the band gap is reduced by the same amount. As the gap is reduced to be smaller than the binding energy, the excitonic order may develop. Note that due to the absence of interlayer tunneling, the device we consider here is equivalent to an equilibrium system, although the bias combined with non-zero interlayer tunneling will drive the system into non-equilibrium steady states [43, 61, 62].

Because the spin-orbital-coupling (SOC) leads to a splitting of the valence band by ~ 470 meV, while the splitting of the conduction band is ~ 20 meV, we include one valence band (v) from WSe₂ and two SOC-split conduction bands (c_1/c_2) from MoSe₂ in Eq. (1), as shown in the left of Fig. 1(b). Moreover, we focus on the K -valley in the following since the K and K' valleys are degenerate in energy [52]. As a dense Brillouin zone (BZ) k -grid is essential to capture the e - h interaction correctly, we adopt the nonuniform BZ sampling method

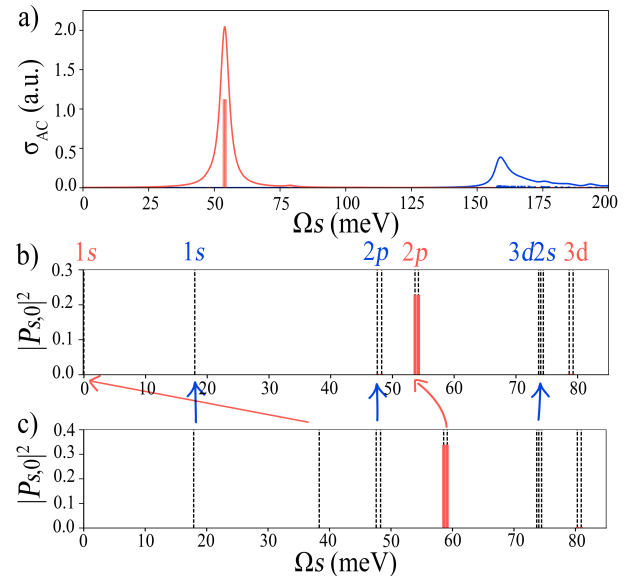


FIG. 2. (a) Optical conductivity along the armchair (AC) direction of the device in Fig. 1(a) in the BEC regime where $E_g = E_b/2$. Red and blue curves are calculated by BSE and IPA respectively with a Lorentzian broadening of 2 meV. (b) The excitation spectrum labeled by corresponding quantum numbers calculated from the BSE in Eq. (7). Red and blue labels are for c_1 - and c_2 -types, respectively. (c) Same as (b) but calculated from TDA. The arrows between (b) and (c) connect the same labels.

[63] using a spherical patch with radius 0.21 Å⁻¹ around the K/K' -valley on a 210×210 k -grid, see Supplemental Material [52, 64–75] for computational details.

Fig. 1(b) shows the normal-state band dispersion ξ_{nk} in the K -valley (left) and the resulting quasiparticle band E_{nk} in the EI state from solving the gap equation (S9) self-consistently, but with a static dielectric screening kept the same as that of the normal state. The only inputs are ξ_{nk} and $V_{vc\mathbf{k},v'c'\mathbf{k}'}$ which are from *ab initio* calculations [49–51]. We tuned the gap by the bias to $E_g = E_b/2$ so that the EI state is in the BEC regime. The originally lower-in-energy c_1 -band is pushed up and the higher c_2 -band is unchanged. In the original band basis, the excitonic order parameter has 2-components: $(\Delta_{vc1k}, \Delta_{vc2k})$. From Fig. 1(c-d), we observe that an *s*-wave excitonic order parameter and non-zero U -matrix element hybridizing the valence band and the c_1 component are developed, while Δ_{vc2k} and U_{vc2k} remain zero.

With the U -matrix from the MF calculation, we build the BSE matrix in Eq. (7) and solve it numerically for the collective excitations. The solutions can be categorized into two groups named the c_1 -type (dominated by A_{vc1k} meaning excitation to the c_1 band) and c_2 -type (dominated by A_{vc2k} meaning excitation to the c_2 band) shown by red and blue labels in Fig. 2b, respectively. The linear optical conductivity can be calculated with the optical transition matrix elements[52]

$$\langle S | \hat{p} | 0 \rangle = \sum_{vc\mathbf{k}} (p'_{vc\mathbf{k}} A_{vc\mathbf{k}}^S + p'_{vc\mathbf{k}} B_{vc\mathbf{k}}^S), \quad (10)$$

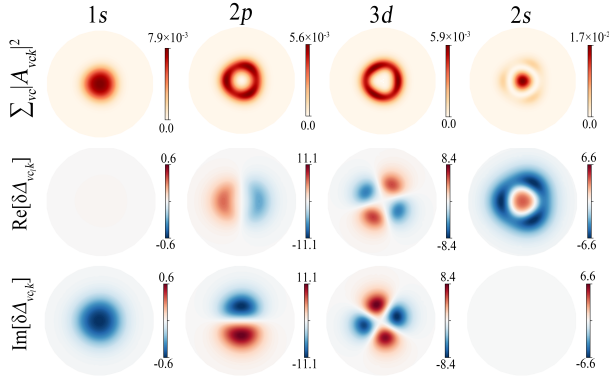


FIG. 3. Plot of $\sum_{vc} |A_{vck}|^2$ and the real and imaginary parts of $\delta\Delta_{vc1k}$ (meV) for a few c_1 -type collective excitations on the momentum plane corresponding to those in Fig. 2.

where

$$p'_{nmk} = \sum_{n'm'} p_{n'm'k} U_{n'k}^{nk*} U_{m'k}^{mk}. \quad (11)$$

Fig. 2 shows the optical conductivity and the excitation spectrum. In Fig. 3 we plot the k -space distribution of $\sum_{vc} |A_{vck}|^2$ and the profiles of order parameter fluctuations for c_1 -type excitations. Because there is an arbitrary phase associated with the Bloch states [76], the order parameter fluctuations in Fig. 3 are plotted as $e^{-i\theta_k} \delta\Delta_{vck}$ with the momentum-dependent phase from the MF order parameter $\Delta_{vck} = e^{i\theta_k} |\Delta_{vck}|$, so that their relative phase is emphasized. From Fig. 3, the angular momenta and radial quantum numbers can be identified for the excitations.

For the c_1 -type excitations, there is a zero-energy solution that corresponds to the phase-mode [17, 39, 40]. It has an s -wave momentum dependence as shown in Fig. 3 and the eigenvector fulfills $|A_{vck}| = |B_{vck}|$. Note that the phase difference between A_{vck} and B_{vck} is related to the gauge freedom in U -matrix. It satisfies $A_{vck} = -B_{vck}$ for a gauge such that U_{nvk} is real. The c_1 -type solutions with non-zero energies are the BaSh modes [39]. All the BaSh modes with non-zero angular momentum are (nearly) doubly degenerate while all the s -wave ones are non-degenerate.

In the normal state, the v and c_1 bands have opposite spin and layer indices, meaning that there should be no interband optical transitions. However, the new bands in the EI state are mixtures between them so that large interband optical matrix elements naturally exist [52]. In the BEC case, these transitions could be viewed as the internal transitions of the excitons from the $1s$ bound state to higher bound states and scattering states. From the approximate rotational symmetry of the bands, all the p -wave BaSh modes are optically active. In Fig. 2, one observes that compared to the independent particle approximation (IPA), the interaction between the quasiparticles rearranges the optical spectra weight from the continuous above-gap excitations to nearly a single strong peak at the $2p$ -mode. The optical activity of the subgap $2p$ -mode may serve as a direct evidence of the presence of excitons in equilibrium. Note that after the Hamiltonian of the electromag-

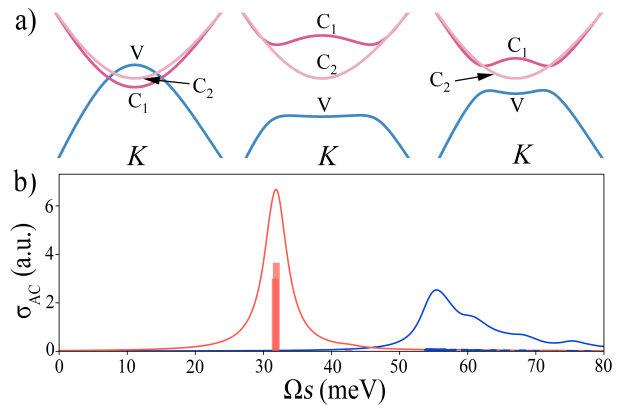


FIG. 4. (a) The BCS EI regime of the device in Fig. 1(a) where the gap is tuned to $E_g \approx -30$ meV. Plotted are the band structures of the normal state (left) and the EI state without (middle) and with (right) updated dielectric screening. Note that the c_2 -band remains unoccupied in this parameter range. (b) Optical conductivity along the AC direction. Red and blue curves are calculated from BSE and IPA respectively with a Lorentzian broadening of 2 meV.

netic field is included, the optically active BaSh modes will hybridize with photons to form BaSh polaritons which exhibit longitudinal-transverse splitting, similar to infrared phonons and bright excitons in solids. In three dimensions, this splitting shows up already at the zero wave vector limits of the modes. In the two-dimensional system we study, this effect shows up only at nonzero wavevectors, see Refs. [39, 42].

The c_2 -type excitations correspond to the fluctuation of $\delta\Delta_{vc2k}$ (see Fig. S1 [52]), and can be classified by the angular quantum in similar ways. From Fig. 2, one observes that all the c_2 -type excitations are optically dark. This is because the excitonic order Δ_{vc1k} does not mix the c_2 band with the other two bands so that the interband optical matrix elements p'_{vc2k} vanish. The non-zero energy (~ 20 meV) of the $1s$ mode originates from the SOC splitting of the two conduction bands, and will become another gapless mode in the limit of zero SOC splitting (see Fig. S2 [52]).

We note that for excitons in semiconductors, one may use the TDA where Π^{AB} and B_{vck} in Eq. (7) are neglected [66]. However, in EIs, the full BSE is necessary to capture the collective modes because the particle-hole pair annihilation channel is an important portion of them. Fig. 2(b-c) show that compared to the result of TDA, the full BSE leads to substantial corrections for the c_1 -type excitations. Nevertheless, TDA is a good approximation for c_2 -type excitations [52].

Finally, in the dilute limit of the BEC case, the excitations are trivially understood as the internal transitions of a single exciton from the $1s$ bound state to higher states. However, many-exciton effect starts to be important even slightly away from the dilute limit, which leads to dramatic shifts of the excitation energies and even their crossings, see Fig. S3 [52]. Therefore, the scheme described in Eqs. 2-9 is indispensable for obtaining the collective excitations in first-principles approaches to EIs beyond the single exciton picture. This point is more obvious in the Bardeen–Cooper–Schrieffer (BCS) regime where the excitons are much larger than the

inter-exciton distance so that the collective excitations depart qualitatively from the BEC case. For example, the order parameter amplitude oscillation exists as the Higgs mode in the BCS weak coupling regime, while it and the phase oscillation become a conjugate pair of the same mode (i.e., the phase-mode) in the BEC case [39, 40]. In Fig. 4, we show a representative result in the BCS regime. The optical conductivity shows that the p -wave BaSh mode is redshift significantly compared to that in the BEC regime. As the exciton density is large, the extra screening from the condensate can be non-negligible. Thus, we updated the dielectric screening using static random phase approximation with an approximated k -sampling [52]. For more accurate results, a self-consistent calculation of the dielectric function with high numerical accuracy is needed in the future.

In conclusion, we presented an *ab initio* approach for computing the collective excitations in EIs. It is also directly applicable to other systems such as charge/spin density waves (with no changes to Eqs. 1-9) [79–81] and BCS superconductors (with a particle-hole transformation of the valence band operators in Eq. (1)) [78]. After integration with existing first-principles software packages, we anticipate this method to enable *ab initio* studies of excited-states in symmetry-broken quantum systems with state-of-the-art accuracy, thus offering concrete guidance for experiments. However, we note that retardation effects of the electron-electron interaction arise in these systems due to either dynamical screening or mediation by phonons. To further increase the accuracy of the first-principles approaches in the future, it is important to go beyond the instantaneous approximation to the interaction. Finally, the BSE formalism is based on the picture of mean field plus Gaussian fluctuations, which works reasonably well for conventional EIs, superconductors and charge/spin density waves in the BCS weak coupling regime. There the validity of the mean field approximation is known to be controlled by a

small Ginzburg parameter [53, 82–84]. Very close to the critical point, or for materials away from the BCS weak coupling regime, the methods addressing strong fluctuations [85] need to be incorporated into *ab initio* approaches in the future.

This work is funded by the National Science and Technology Major Project (Grants No. 2023ZD0120702), Basic Research Program of Jiangsu (Grants No. BK20240395), the National Natural Science Foundation of China (Grants No. 12374291 and No. 12421004), the National Key Research and Development Program of China (2022YFA1204700), and Beijing Natural Science Foundation (Z240005). Calculations were performed on Sugon HPC clusters equipped with HY-GON X86 32-core processors (2.5 GHz) and at the Beijing Super Cloud Computing Center. We thank Y. Murakami, D. Golež, Y. Xu and C. Wang for helpful discussions.

Appendix A

Here we derive the BSE with zero-momentum in Eq. (7) and Eq. (8) using the EOM method in the quasiparticle representation. EOM method [55, 56] requires evaluation of commutation $[H, \gamma_{ck}^\dagger \gamma_{vk}]$ and $[H, \gamma_{vk}^\dagger \gamma_{ck}]$. For the MF Hamiltonian, we have

$$\begin{aligned} \sum_{c'k'} [E_{c'k'} \gamma_{c'k'}^\dagger \gamma_{c'k'}, \gamma_{ck}^\dagger \gamma_{vk}] &= E_{ck} \gamma_{ck}^\dagger \gamma_{vk}, \\ \sum_{v'k'} [E_{v'k'} \gamma_{v'k'}^\dagger \gamma_{v'k'}, \gamma_{ck}^\dagger \gamma_{vk}] &= -E_{vk} \gamma_{ck}^\dagger \gamma_{vk}. \end{aligned} \quad (\text{A1})$$

For the fluctuation Hamiltonian, we use Eq. (5) to write out explicitly the particle-hole scattering matrix elements first, $\sum_{vck, v'c'k'} \Pi_{vck, v'c'k'}^+ \gamma_{v'k'}^\dagger \gamma_{c'k'} \gamma_{c'k'}^\dagger \gamma_{v'k'} \gamma_{vk}^\dagger \gamma_{vk}$ and $\sum_{vck, v'c'k'} \Pi_{vck, v'c'k'}^- \gamma_{v'k'}^\dagger \gamma_{c'k'} \gamma_{c'k'}^\dagger \gamma_{v'k'} \gamma_{vk}^\dagger \gamma_{vk}$ where

$$\begin{aligned} \Pi_{vck, v'c'k'}^+ &= - \sum_{v_1 c_1, v'_1 c'_1} \left(V_{v_1 c_1 k, v'_1 c'_1 k'} U_{c'_1 k'}^{c'k'*} U_{v'_1 k'}^{v'k'*} U_{v_1 k}^{vk*} U_{c_1 k}^{ck} + V_{v'_1 c'_1 k', v_1 c_1 k} U_{c_1 k}^{vk*} U_{v_1 k}^{ck} U_{v'_1 k'}^{c'k'*} U_{c'_1 k'}^{v'k'*} \right), \\ \Pi_{vck, v'c'k'}^- &= - \sum_{v_1 c_1, v'_1 c'_1} V_{v_1 c_1 k, v'_1 c'_1 k'} U_{c_1 k}^{ck} U_{v_1 k}^{vk*} U_{v'_1 k'}^{c'k'*} U_{c'_1 k'}^{v'k'*}. \end{aligned} \quad (\text{A2})$$

Next, taking the approximation $[\gamma_{v'k'}^\dagger \gamma_{c'k'}, \gamma_{ck}^\dagger \gamma_{vk}] \approx \delta_{vck, v'c'k'} \gamma_{v'k'}^\dagger \gamma_{c'k'} \gamma_{ck}^\dagger \gamma_{vk}$, we have

$$\begin{aligned} \sum_{vck, v'c'k'} \Pi_{vck, v'c'k'}^+ [\gamma_{c'k'}^\dagger \gamma_{v'k'} \gamma_{vk}^\dagger \gamma_{ck}, \gamma_{ck}^\dagger \gamma_{vk}] &= \sum_{v'c'k'} \Pi_{v_1 c_1 k_1, v'c'k'}^+ \gamma_{c'k'}^\dagger \gamma_{v'k'} \gamma_{v'k'}^\dagger \gamma_{c'k'}, \\ \sum_{vck, v'c'k'} \Pi_{vck, v'c'k'}^- [\gamma_{v'k'}^\dagger \gamma_{c'k'} \gamma_{vk}^\dagger \gamma_{ck}, \gamma_{ck}^\dagger \gamma_{vk}] &= \sum_{v'c'k'} (\Pi_{v_1 c_1 k_1, v'c'k'}^- + \Pi_{v_1 c_1 k_1, v'c'k'}^{-T}) \gamma_{v'k'}^\dagger \gamma_{c'k'}. \end{aligned} \quad (\text{A3})$$

Finally, inserting the commutations of Eq. (A1) and Eq. (A3) in the EOM,

$$\begin{aligned} \langle S | [H, \gamma_{ck}^\dagger \gamma_{vk}] | 0 \rangle &= \Omega_S A_{vck}^S, \\ \langle S | [H, \gamma_{vk}^\dagger \gamma_{ck}] | 0 \rangle &= \Omega_S B_{vck}^S, \end{aligned} \quad (\text{A4})$$

we obtain the BSE in the matrix form of Eq. (7), where $A_{vck}^S = \langle S | \gamma_{ck}^\dagger \gamma_{vk} | 0 \rangle$ and $B_{vck}^S = \langle S | \gamma_{vk}^\dagger \gamma_{ck} | 0 \rangle$ which is normalized by $\sum_{vck} (A_{vck}^{S'} A_{vck}^{S*} - B_{vck}^{S'} B_{vck}^{S*}) = \delta_{SS'}$. For phase mode where $|A_{vck}| = |B_{vck}|$, we can normalize it with $\sum_{vck} |A_{vck}|^2 = 1$ [75]. The BSE kernel in Eq. (8) can

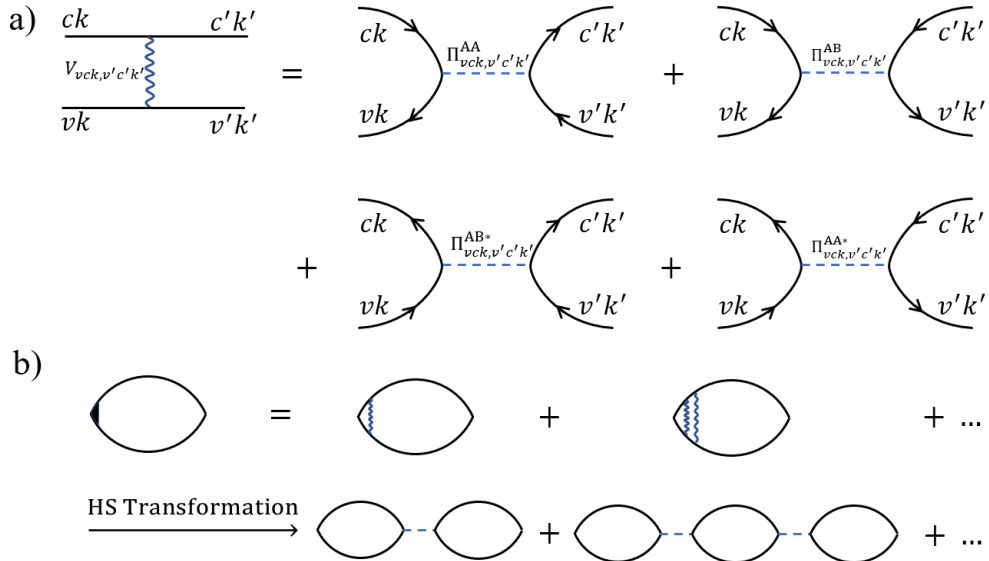


FIG. 5. (a) Feynman diagrams for the e - h propagator which yields the BSE. The two incoming legs may be viewed as the creation of a boson by a_S^\dagger , so that this diagram is actually the self energy of the bosonic propagator. Black solid lines are electronic propagators, which are corrected by the mean field if the system is in the broken symmetry phase. We use the blue wavy line to represent the interband interaction $V_{vck, v'c'k'}$ that includes both the direct and exchange interactions. The blue dashed line represents the same interaction, but explicitly decomposed in the e - h and anti- e - h channels in the diagonalized band basis. (b) Representation of collective modes in terms of bosonic propagators. The first line is the bosonic propagator expressed in terms of the original interband interaction $V_{vck, v'c'k'}$. The collective modes are contained in the vertex [10, 77]. The second line are the equivalent diagrams after the Hubbard-Stratonovich transformation, where blue dashed lines are the propagators of the bosonic field that mediates the interaction $V_{vck, v'c'k'}$ [39, 78].

be deduced from $\Pi^{AA} = \Pi^+$, $\Pi^{BB} = \Pi^{+*}$ and $\Pi^{AB} = \Pi^- + \Pi^{-T}$, $\Pi^{BA} = \Pi^{-*} + \Pi^{-*T}$.

The BSE can also be understood by the Feynman diagrams shown in Fig. 5(a). The diagram on the left of Fig. 5(a) is viewed as the self energy for the propagator $G(\omega)$ of the zero center-of-mass-momentum boson $a_S^\dagger = \sum_{vck} (A_{vck}^{S*} \gamma_{ck}^\dagger \gamma_{vk} - B_{vck}^{S*} \gamma_{vk}^\dagger \gamma_{ck})$. Expanded in the (A, B)

basis gives the four diagrams on the right, which is just the $\hat{\Pi}$ matrix in Eq. (7). Adding this self energy to the propagator of the free e - h (and anti- e - h) pairs, one obtains

$$G(\omega) = \left[\omega - \begin{pmatrix} K & 0 \\ 0 & -K \end{pmatrix} - \hat{\Pi} \right]^{-1}. \quad (\text{A5})$$

Its pole condition gives the BSE in Eq. (7). Note that the off diagonal elements of $\hat{\Pi}$ mix e - h and anti- e - h pairs.

[1] G. Onida, L. Reining, and Rubio, Electronic excitations: density-functional versus many-body Green's-function approaches, *Rev. Mod. Phys.* **74**, 601 (2002).

[2] L. N. Oliveira, E. K. U. Gross, and W. Kohn, Density-functional theory for superconductors, *Phys. Rev. Lett.* **60**, 2430 (1988).

[3] S. Kurth, M. Marques, M. Lüders, and E. K. U. Gross, Local density approximation for superconductors, *Phys. Rev. Lett.* **83**, 2628 (1999).

[4] M. Lüders, M. A. L. Marques, N. N. Lathiotakis, A. Floris, G. Profeta, L. Fast, A. Continenza, S. Massidda, and E. K. U. Gross, *Ab initio* theory of superconductivity. I. density functional formalism and approximate functionals, *Phys. Rev. B* **72**, 024545 (2005).

[5] D. Varsano, S. Sorella, D. Sangalli, M. Barborini, S. Corni, E. Molinari, and M. Rontani, Carbon nanotubes as excitonic insulators, *Nat. Commun.* **8**, 1461 (2017).

[6] S. Conti, A. Perali, F. M. Peeters, and D. Neilson, Multicomponent screening and superfluidity in gapped electron-hole double bilayer graphene with realistic bands, *Phys. Rev. B* **99**, 144517 (2019).

[7] D. Varsano, M. Palummo, E. Molinari, and M. Rontani, A monolayer transition-metal dichalcogenide as a topological excitonic insulator, *Nat. Nanotechnol.* **15**, 367–372 (2020).

[8] H.-Y. Chen, T. Nomoto, and R. Arita, Development of an *ab initio* method for exciton condensation and its application to TiSe_2 , *Phys. Rev. Res.* **5**, 043183 (2023).

[9] A. W. Anderson, Random-phase approximation in the theory of superconductivity, *Phys. Rev.* **112**, 1900 (1958).

[10] A. Bardasis and J. R. Schrieffer, Excitons and plasmons in superconductors, *Phys. Rev.* **121**, 1050 (1961).

[11] L. V. Keldysh and Y. V. Kopaev, Possible instability of the semimetallic state toward Coulomb interaction, *Sov. Phys. Solid State* **6**, 2219 (1965).

[12] D. Jerome, T. M. Rice, and W. Kohn, Excitonic insulator, *Phys. Rev. B* **158**, 462 (1967).

[13] T. Kaneko and Y. Ohta, A new era of excitonic insulators, *J.*

Phys. Soc. Jpn. **94**, 012001 (2025).

[14] T. Portengen, T. Östreich, and L. J. Sham, Theory of electronic ferroelectricity, Phys. Rev. B **54**, 17452 (1996).

[15] B. Zenker, H. Fehske, and H. Beck, Fate of the excitonic insulator in the presence of phonons, Phys. Rev. B **90**, 195118 (2014).

[16] G. Mazza, M. Rösner, L. Windgärtter, S. Latini, H. Hübener, A. J. Millis, A. Rubio, and A. Georges, Nature of symmetry breaking at the excitonic insulator transition: Ta_2NiSe_5 , Phys. Rev. Lett. **124**, 197601 (2020).

[17] D. Golež, Z. Sun, Y. Murakami, A. Georges, and A. J. Millis, Nonlinear spectroscopy of collective modes in an excitonic insulator, Phys. Rev. Lett. **125**, 257601 (2020).

[18] Z. Sun, T. Kaneko, D. Golež, and A. J. Millis, Second-order Josephson effect in excitonic insulators, Phys. Rev. Lett. **127**, 127702 (2021).

[19] T. Kaneko, Z. Sun, Y. Murakami, D. Golež, and A. J. Millis, Bulk photovoltaic effect driven by collective excitations in a correlated insulator, Phys. Rev. Lett. **127**, 127402 (2021).

[20] Y. Wakisaka, T. Sudayama, K. Takubo, T. Mizokawa, M. Arita, H. Namatame, M. Taniguchi, N. Katayama, M. Nohara, and H. Takagi, Excitonic insulator state in Ta_2NiSe_5 probed by photoemission spectroscopy, Phys. Rev. Lett. **103**, 026402 (2009).

[21] Y. F. Lu, H. Kono, T. I. Larkin, A. W. Rost, T. Takayama, A. V. Boris, B. Keimer, and H. Takagi, Zero-gap semiconductor to excitonic insulator transition in Ta_2NiSe_5 , Nat. Commun. **8**, 14408 (2017).

[22] D. Werdehausen, T. Takayama, M. Höppner, G. Albrecht, A. W. Rost, Y. Lu, D. Manske, H. Takagi, and S. Kaiser, Coherent order parameter oscillations in the ground state of the excitonic insulator Ta_2NiSe_5 , Sci. Adv. **4**, eaap8652 (2018).

[23] H. Ning, O. Mehio, M. Buchhold, T. Kurumaji, G. Refael, J. G. Checkelsky, and D. Hsieh, Signatures of ultrafast reversal of excitonic order in Ta_2NiSe_5 , Phys. Rev. Lett. **125**, 267602 (2020).

[24] K. Kim, H. Kim, J. Kim, C. Kwon, J. S. Kim, and B. J. Kim, Direct observation of excitonic instability in Ta_2NiSe_5 , Nat. Commun. **12**, 1969 (2021).

[25] P. A. Volkov, M. Ye, H. Lohani, I. Feldman, A. Kanigel, and G. Blumberg, Failed excitonic quantum phase transition in $Ta_2Ni(Se_{1-x}S_x)_5$, Phys. Rev. B **104**, L241103 (2021).

[26] H. M. Bretscher, P. Andrich, Y. Murakami, D. Golež, B. Remez, P. Telang, A. Singh, L. Harnagea, N. R. Cooper, A. J. Millis, P. Werner, A. K. Sood, and A. Rao, Imaging the coherent propagation of collective modes in the excitonic insulator Ta_2NiSe_5 at room temperature, Sci. Adv. **7**, eabd6147 (2021).

[27] K. Fukutani, R. Stania, C. Il Kwon, J. S. Kim, K. J. Kong, J. Kim, and H. W. Yeom, Direct observation of excitonic instability in Ta_2NiSe_5 , Nat. Phys. **17**, 1024 (2021).

[28] D. Golež, S. K. Y. Dufresne, M.-J. Kim, F. Boschini, H. Chu, Y. Murakami, G. Levy, A. K. Mills, S. Zhdanovich, M. Isobe, H. Takagi, S. Kaiser, P. Werner, D. J. Jones, A. Georges, A. Damascelli, and A. J. Millis, Unveiling the underlying interactions in Ta_2NiSe_5 from photoinduced lifetime change, Phys. Rev. B **106**, L121106 (2022).

[29] Y. Jia, P. Wang, C.-L. Chiu, Z. Song, G. Yu, B. Jäck, S. Lei, S. Klemenz, F. A. Cevallos, M. Onyszczak, and *et al.*, Evidence for a monolayer excitonic insulator, Nat. Phys. **18**, 87 (2022).

[30] B. Sun, W. Zhao, T. Palomaki, Z. Fei, E. Runburg, P. Malinowski, X. Huang, J. Cenker, Y.-T. Cui, J.-H. Chu, and *et al.*, Evidence for equilibrium exciton condensation in monolayer WTe_2 , Nat. Phys. **18**, 94 (2022).

[31] M. S. Hossain, Z.-J. Cheng, Y.-X. Jiang, T. A. Cochran, S.-B. Zhang, H. Wu, X. Liu, X. Zheng, G. Cheng, B. Kim, and *et al.*, Topological excitonic insulator with tunable momentum order, Nat. Phys. **21**, 1250 (2025).

[32] Z. Wang, D. A. Rhodes, K. Watanabe, T. Taniguchi, J. C. Hone, J. Shan, and K. F. Mak, Evidence of high-temperature exciton condensation in two-dimensional atomic double layers, Nature **574**, 76 (2019).

[33] L. Ma, P. X. Nguyen, Z. Wang, Y. Zeng, K. Watanabe, T. Taniguchi, A. H. MacDonald, K. F. Mak, and J. Shan, Strongly correlated excitonic insulator in atomic double layers, Nature **598**, 585 (2021).

[34] Z. Zhang, E. C. Regan, D. Wang, W. Zhao, S. Wang, M. Sayyad, K. Yumigeta, K. Watanabe, T. Taniguchi, S. Tongay, and *et al.*, Correlated interlayer exciton insulator in heterostructures of monolayer WSe_2 and moiré WS_2/WSe_2 , Nat. Phys. **18**, 1214 (2022).

[35] R. Wang, T. A. Sedrakyan, B. Wang, L. Du, and R.-R. Du, Excitonic topological order in imbalanced electron-hole bilayers, Nature **619**, 57 (2023).

[36] P. X. Nguyen, L. Ma, R. Chaturvedi, K. Watanabe, T. Taniguchi, J. Shan, and K. F. Mak, Perfect Coulomb drag in a dipolar excitonic insulator, Science **388**, 274 (2025).

[37] P. X. Nguyen, R. Chaturvedi, B. Zou, K. Watanabe, T. Taniguchi, A. H. MacDonald, K. F. Mak, and J. Shan, Quantum oscillations in a dipolar excitonic insulator, Nat. Mater. **00**, 00 (2025).

[38] F.-C. Wu, F. Xue, and A. H. MacDonald, Theory of two-dimensional spatially indirect equilibrium exciton condensates, Phys. Rev. B **92**, 165121 (2015).

[39] Z. Sun and A. J. Millis, Bardasis-schrieffer polaritons in excitonic insulators, Phys. Rev. B **102**, 041110(R) (2020).

[40] Y. Murakami, D. Golež, T. Kaneko, A. Koga, A. J. Millis, and P. Werner, Collective modes in excitonic insulators: Effects of electron-phonon coupling and signatures in the optical response, Phys. Rev. B **101**, 195118 (2020).

[41] F. Xue, F. Wu, and A. H. MacDonald, Higgs-like modes in two-dimensional spatially indirect exciton condensates, Phys. Rev. B **102**, 075136 (2020).

[42] Y. Shao, H. Shi, and X. Dai, Electromagnetic responses of bilayer excitonic insulators, arXiv:2509.02142v1 (2025).

[43] Z. Sun, Y. Murakami, F. Xuan, T. Kaneko, D. Golež, and A. J. Millis, Dynamical exciton condensates in biased electron-hole bilayers, Phys. Rev. Lett. **133**, 217002 (2024).

[44] F.-C. Wu, F. Xue, and A. H. MacDonald, Theory of two-dimensional spatially indirect equilibrium exciton condensates, Phys. Rev. B **92**, 165121 (2015).

[45] F. Xue, F. Wu, and A. H. MacDonald, Higgs-like modes in two-dimensional spatially indirect exciton condensates, Phys. Rev. B **102**, 075136 (2020).

[46] B. Chatterjee, J. Mravlje, and D. Golež, Collective modes and Raman response in Ta_2NiSe_5 , Phys. Rev. B **111**, L121106 (2025).

[47] L. V. Keldysh and A. N. Kozlov, Collective properties of excitons in semiconductors, Sov. Phys. JETP **40**, 755 (1968).

[48] Z. Fang, J. Ruan, G. Sethi, C. Hu, and S. Louie, *Ab initio* study of exciton insulator phase: Emergent *p*-wave spin textures from spontaneous excitonic condensation, arXiv:2503.11563v1 (2025).

[49] P. Giannozzi, S. Baroni, N. Bonini, M. Calandra, B. Car, C. Cavazzoni, D. Ceresoli, G. L. Chiarotti, M. Cococcioni, and *et al.*, QUANTUM ESPRESSO: a modular and open-source software project for quantum simulations of materials, J. Phys. Condens. Matter **21**, 395502 (2009).

[50] P. Giannozzi, O. Andreussi, T. Brumme, O. Bunau, M. B. Nardelli, M. Calandra, R. Car, C. Cavazzoni, D. Ceresoli, M. Cococcioni, and *et al.*, Advanced capabilities for materials

modelling with Quantum ESPRESSO, *J. Phys. Condens. Matter* **29**, 465901 (2017).

[51] J. Deslippe, G. Samsonidze, D. A. Strubbe, M. Jain, M. L. Cohen, and S. G. Louie, BerkeleyGW: a massively parallel computer package for the calculation of the quasiparticle and optical properties of materials and nanostructures, *Comput. Phys. Commun.* **183**, 1269 (2012).

[52] See Supplemental Materials for derivations of Eqs. 2-9, effects from other many-body interactions, dielectric screening of exciton condensate and computational details, which includes Refs. 64-75.

[53] P. Coleman, *Introduction to Many-Body Physics* (Cambridge University Express, 2015).

[54] A. Altland and B. Simons, *Condensed Matter Field Theory* (Cambridge University Express, 2023).

[55] D. J. Rowe, Equations-of-motion method and the extended shell model, *Rev. Mod. Phys.* **40**, 153 (1968).

[56] A. L. Fetter and J. D. Walecka, *Quantum Theory of Many-Particle Systems*. (McGraw-Hill, 1971).

[57] J.-H. Choi, P. Cui, H. Lan, and Z. Zhang, Linear scaling of the exciton binding energy versus the band gap of two-dimensional materials, *Phys. Rev. Lett.* **115**, 066403 (2015).

[58] M. M. Fogler, L. V. Butov, and K. S. Novoselov, High-temperature superfluidity with indirect excitons in van der Waals heterostructures, *Nat. Commun.* **5**, 4555 (2014).

[59] M. M. Ugeda, A. J. Bradley, S. F. Shi, F. H. da Jornada, Y. Zhang, and *et. al.*, Giant bandgap renormalization and excitonic effects in a monolayer transition metal dichalcogenide semiconductor, *Nat. Mater.* **13**, 1091 (2014).

[60] F. Xuan, Y. Chen, and S. Y. Quek, Quasiparticle levels at large interface systems from many-body perturbation theory: The XAF-GW methods, *J. Chem. Theory Comput.* **15**, 3824 (2019).

[61] Y. Zeng, V. Crépel, and A. J. Millis, Keldysh field theory of dynamical exciton condensation transitions in nonequilibrium electron-hole bilayers, *Phys. Rev. Lett.* **132**, 266001 (2024).

[62] A. Osterkorn, Y. Murakami, T. Kaneko, Z. Sun, A. J. Millis, and D. Golež, Optical signatures of dynamical excitonic condensates, *Phys. Rev. Lett.* **135**, 106902 (2025).

[63] A. M. Alvertis, A. Champagne, M. D. Ben, F. H. d. Jornada, D. Y. Qiu, M. R. Filip, and J. B. Neaton, Importance of nonuniform brillouin zone sampling for *ab initio* Bethe-Salpeter equation calculations of exciton binding energies in crystalline solids, *Phys. Rev. B* **108**, 235117 (2023).

[64] M. S. Hybertsen and S. G. Louie, Electron correlation in semiconductors and insulators: Band gaps and quasiparticle energies, *Phys. Rev. B* **34**, 5390 (1986).

[65] M. S. Hybertsen and S. G. Louie, *Ab initio* static dielectric matrices from the density-functional approach. I. formulation and application to semiconductors and insulators, *Phys. Rev. B* **35**, 5585 (1987).

[66] M. Rohlfing and S. G. Louie, Electron-hole excitations and optical spectra from first principles, *Phys. Rev. B* **62**, 4927 (2000).

[67] D. R. Hamann, Optimized norm-conserving vanderbilt pseudopotentials, *Phys. Rev. B* **88**, 085117 (2013).

[68] M. Schlipf and F. Gygi, Optimization algorithm for the generation of oncv pseudopotentials, *Comput. Phys. Commun.* **196**, 36 (2015).

[69] J. P. Perdew, K. Burke, and M. Ernzerhof, Generalized gradient approximation made simple, *Phys. Rev. Lett.* **77**, 3865 (1996).

[70] S. Grimme, Semiempirical GGA-Type density functional constructed with a long-range dispersion correction, *J. Comput. Chem.* **27**, 1787 (2006).

[71] S. Ismail-Beigi, Truncation of periodic image interactions for confined systems, *Phys. Rev. B* **73**, 233103 (2006).

[72] N. N. Bogoliubov, A new method in the theory of superconductivity, *J. Exptl. Theoret. Phys. U.S.S.R.* **34**, 65 (1958).

[73] N. N. Bogoliubov, A new method in the theory of superconductivity, *Sov. Phys. JETP* **34**, 41 (1958).

[74] S. Dong, Y. Chen, H. Qu, W.-K. Lou, and K. Chang, Topological exciton density wave in monolayer WSe₂, *Phys. Rev. Lett.* **134**, 066602 (2025).

[75] D. J. Thouless, Vibrational states of nuclei in the random phase approximation, *Nucl. Phys.* **22**, 78 (1961).

[76] F. Xuan and S. Y. Quek, Valley Zeeman effect and Landau levels in two-dimensional transition metal dichalcogenides, *Phys. Rev. Res.* **2**, 033256 (2020).

[77] P. B. Littlewood and C. M. Varma, Amplitude collective modes in superconductors and their coupling to charge-density waves, *Phys. Rev. B* **26**, 4883 (1982).

[78] Z. Sun, M. M. Fogler, D. N. Basov, and A. J. Millis, Collective modes and terahertz near-field response of superconductors, *Phys. Rev. Res.* **2**, 023413 (2020).

[79] G. Grüner, The dynamics of charge-density waves, *Rev. Mod. Phys.* **60**, 1129 (1988).

[80] G. Grüner, The dynamics of spin-density waves, *Rev. Mod. Phys.* **66**, 1 (1994).

[81] Z. Sun, Floquet engineering of many-body states by the ponderomotive potential, *Phys. Rev. B* **110**, 104301 (2024).

[82] V. L. Ginzburg, Some remarks on phase transitions of the 2nd kind and the microscopic theory of ferroelectric materials, *Sov. Phys. Solid State* **2**, 1824 (1961).

[83] N. Goldenfeld, *Lectures on Phase Transitions and the Renormalization Group* (CRC Press, Boca Raton, FL, 2018).

[84] Z. Sun and A. J. Millis, Transient trapping into metastable states in systems with competing orders, *Phys. Rev. X* **10**, 021028 (2020).

[85] K. G. Wilson, The renormalization group: Critical phenomena and the Kondo problem, *Rev. Mod. Phys.* **47**, 773 (1975).

Supplemental Material for: *Ab initio* Approach to Collective Excitations in Excitonic Insulators

Fengyuan Xuan,^{1,*} Jiexi Song,¹ and Zhiyuan Sun^{2,3,†}

¹*Suzhou Laboratory, Suzhou, 215123, China*

²*State Key Laboratory of Low-Dimensional Quantum Physics and Department of Physics, Tsinghua University, Beijing 100084, P. R. China*

³*Frontier Science Center for Quantum Information, Beijing 100084, P. R. China*

I. SUPPLEMENTARY NOTES

A. Partition of the mean-field and fluctuation Hamiltonian

In this section, we provide derivation for the partition of the mean-field (MF) and fluctuation Hamiltonian. The starting point is the Hamiltonian with the electron-hole (*e-h*) interactions [11, 12, 47],

$$H = \sum_{ck} \xi_{ck} c_{ck}^\dagger c_{ck} + \sum_{vk} \xi_{vk} c_{vk}^\dagger c_{vk} - \sum_{vck, v'c'k', Q} V_{vck, v'c'k'}^Q c_{c'k'+Q}^\dagger c_{v'k'} c_{vk}^\dagger c_{ck+Q}, \quad (\text{S1})$$

where $V_{vck, v'c'k'}^Q$ consists of direct and exchange interactions [64–66],

$$V_{vck, v'c'k'}^Q = \langle \psi_{c'k'+Q} \psi_{vk} | W(r, r', \omega) | \psi_{ck+Q} \psi_{v'k'} \rangle - \langle \psi_{c'k'+Q} \psi_{vk} | \frac{1}{|r - r'|} | \psi_{v'k'} \psi_{ck+Q} \rangle. \quad (\text{S2})$$

We next proceed with the zero-momentum case (Eq. 1 in the maintext) and omit the label Q . The formalism for *e-h* pairing with non-zero center-of-mass momenta is similar. We note that for $Q = 0$ pairing, the $V_{vck, v'c'k'}^Q$ with finite- Q contribute to collective excitations with non-zero momenta. The other two-body interaction terms such as electron-electron (*e-e*), hole-hole (*h-h*) interactions and intrinsic interband tunneling terms are neglected here and will be discussed in Section D.

By separating $c_{vk}^\dagger c_{ck}$ into its expectation value, $\varphi_{vck} \equiv \langle c_{vk}^\dagger c_{ck} \rangle$, in the symmetry-broken ground state and a fluctuation term, the *e-h* interaction is partitioned as

$$\begin{aligned} - \sum_{vck, v'c'k'} V_{vck, v'c'k'} c_{c'k'}^\dagger c_{v'k'} c_{vk}^\dagger c_{ck} &= - \sum_{vck, v'c'k'} V_{vck, v'c'k'} \left(\varphi_{v'c'k'}^* + c_{c'k'}^\dagger c_{v'k'} - \varphi_{v'c'k'}^* \right) \left(\varphi_{vck} + c_{vk}^\dagger c_{ck} - \varphi_{vck} \right) \\ &= H_0 - \sum_{vck} \Delta_{vck}^* c_{vk}^\dagger c_{ck} - \sum_{vck} c_{ck}^\dagger c_{vk} \Delta_{vck} + H_{\text{fluc}}, \end{aligned} \quad (\text{S3})$$

where $\Delta_{vck} = \sum_{v'c'k'} V_{v'c'k', vck} \varphi_{v'c'k'}$, H_0 and H_{fluc} are,

$$H_0 = \sum_{vck, v'c'k'} V_{vck, v'c'k'} \varphi_{vck} \varphi_{v'c'k'}^*, \quad (\text{S4})$$

$$H_{\text{fluc}} = - \sum_{vck, v'c'k'} V_{vck, v'c'k'} \left(c_{c'k'}^\dagger c_{v'k'} - \varphi_{v'c'k'}^* \right) \left(c_{vk}^\dagger c_{ck} - \varphi_{vck} \right). \quad (\text{S5})$$

Therefore, the MF Hamiltonian reads

$$\begin{aligned}
H_{\text{MF}} &= H_0 + \sum_{ck} \xi_{ck} c_{ck}^\dagger c_{ck} + \sum_{vk} \xi_{vk} c_{vk}^\dagger c_{vk} - \sum_{vck} \Delta_{vck}^* c_{vk}^\dagger c_{ck} - \sum_{vck} c_{ck}^\dagger c_{vk} \Delta_{vck} \\
&= H_0 + \sum_k [\dots c_{c_2k}^\dagger c_{c_1k}^\dagger c_{v_1k}^\dagger c_{v_2k}^\dagger \dots] h_k \begin{bmatrix} \dots \\ c_{c_2k} \\ c_{c_1k} \\ c_{v_1k} \\ c_{v_2k} \\ \dots \end{bmatrix} \\
&= H_0 + \sum_k [\dots c_{c_2k}^\dagger c_{c_1k}^\dagger c_{v_1k}^\dagger c_{v_2k}^\dagger \dots] \begin{bmatrix} \dots & \dots & \dots & \dots & \dots & \dots \\ \dots & \xi_{c_2k} & 0 & -\Delta_{v_1c_2k} & -\Delta_{v_2c_2k} & \dots \\ \dots & 0 & \xi_{c_1k} & -\Delta_{v_1c_1k} & -\Delta_{v_2c_1k} & \dots \\ \dots & -\Delta_{v_1c_2k}^* & -\Delta_{v_1c_1k}^* & \xi_{v_1k} & 0 & \dots \\ \dots & -\Delta_{v_2c_2k}^* & -\Delta_{v_2c_1k}^* & 0 & \xi_{v_2k} & \dots \\ \dots & \dots & \dots & \dots & \dots & \dots \end{bmatrix} \begin{bmatrix} \dots \\ c_{c_2k} \\ c_{c_1k} \\ c_{v_1k} \\ c_{v_2k} \\ \dots \end{bmatrix} \quad (S6) \\
&= H_0 + \sum_k [\dots c_{c_2k}^\dagger c_{c_1k}^\dagger c_{v_1k}^\dagger c_{v_2k}^\dagger \dots] U \begin{bmatrix} \dots & \dots & \dots & \dots & \dots & \dots \\ \dots & E_{c_2k} & 0 & 0 & 0 & \dots \\ \dots & 0 & E_{c_1k} & 0 & 0 & \dots \\ \dots & 0 & 0 & E_{v_1k} & 0 & \dots \\ \dots & 0 & 0 & 0 & E_{v_2k} & \dots \\ \dots & \dots & \dots & \dots & \dots & \dots \end{bmatrix} U^\dagger \begin{bmatrix} \dots \\ c_{c_2k} \\ c_{c_1k} \\ c_{v_1k} \\ c_{v_2k} \\ \dots \end{bmatrix} \\
&= H_0 + \sum_k [\dots \gamma_{c_2k}^\dagger \gamma_{c_1k}^\dagger \gamma_{v_1k}^\dagger \gamma_{v_2k}^\dagger \dots] \begin{bmatrix} \dots & \dots & \dots & \dots & \dots & \dots \\ \dots & E_{c_2k} & 0 & 0 & 0 & \dots \\ \dots & 0 & E_{c_1k} & 0 & 0 & \dots \\ \dots & 0 & 0 & E_{v_1k} & 0 & \dots \\ \dots & 0 & 0 & 0 & E_{v_2k} & \dots \\ \dots & \dots & \dots & \dots & \dots & \dots \end{bmatrix} \begin{bmatrix} \dots \\ \gamma_{c_2k} \\ \gamma_{c_1k} \\ \gamma_{v_1k} \\ \gamma_{v_2k} \\ \dots \end{bmatrix} \\
&= H_0 + \sum_{ck} E_{ck} \gamma_{ck}^\dagger \gamma_{ck} + \sum_{vk} E_{vk} \gamma_{vk}^\dagger \gamma_{vk}.
\end{aligned}$$

In the above equation, the unitary transformation U -matrix with each column built by the eigenvectors of h_k (Eq. 3 in the maintext) relates the c -operator for electrons with the γ -operator for quasiparticles [72, 73],

$$\begin{bmatrix} \dots \\ c_{c_2k} \\ c_{c_1k} \\ c_{v_1k} \\ c_{v_2k} \\ \dots \end{bmatrix} = \begin{bmatrix} \dots & \dots & \dots & \dots & \dots & \dots \\ \dots & U_{c_2k}^{nk} & \dots & \dots & U_{c_2k}^{mk} & \dots \\ \dots & U_{c_1k}^{nk} & \dots & \dots & U_{c_1k}^{mk} & \dots \\ \dots & U_{v_1k}^{nk} & \dots & \dots & U_{v_1k}^{mk} & \dots \\ \dots & U_{v_2k}^{nk} & \dots & \dots & U_{v_2k}^{mk} & \dots \\ \dots & \dots & \dots & \dots & \dots & \dots \end{bmatrix} \begin{bmatrix} \dots \\ \gamma_{c_2k} \\ \gamma_{c_1k} \\ \gamma_{v_1k} \\ \gamma_{v_2k} \\ \dots \end{bmatrix} = U \begin{bmatrix} \dots \\ \gamma_{c_2k} \\ \gamma_{c_1k} \\ \gamma_{v_1k} \\ \gamma_{v_2k} \\ \dots \end{bmatrix}. \quad (S7)$$

Using the γ -operator, the MF ground state can be constructed by

$$|\text{MF}\rangle = \prod_{vk} \gamma_{vk}^\dagger c_{vk} |\text{HF}\rangle = \prod_{vk} \left(\sum_n \tilde{U}_{vk}^{nk*} c_{nk}^\dagger \right) c_{vk} |\text{HF}\rangle = \prod_{vk} \left(U_{vk}^{vk} + \sum_c U_{ck}^{vk} c_{ck}^\dagger c_{vk} \right) |\text{HF}\rangle, \quad (S8)$$

where $\tilde{U}_{mk}^{nk} = U_{mk}^{nk*}$, and $|\text{HF}\rangle$ is the conventional Hartree-Fock ground state for semiconductors. For the BCS regime, $|\text{MF}\rangle$ can be written in the same form if the valence and conduction bands are defined according to the Fermi surface. Note that we define c/v according to the original band indices before applying the bias voltage in the maintext.

The self-consistent gap equation reads

$$\Delta_{vck} = \langle \text{MF} | \sum_{v'c'k'} V_{v'c'k',vck} c_{v'k'}^\dagger c_{c'k'} | \text{MF} \rangle = \sum_{v'c'k'} V_{v'c'k',vck} \langle \text{MF} | c_{v'k'}^\dagger c_{c'k'} | \text{MF} \rangle = \sum_{v'c'k'} V_{v'c'k',vck} \varphi_{v'c'k'}, \quad (S9)$$

where $\varphi_{vck} \equiv \langle c_{vk}^\dagger c_{ck} \rangle = \sum_{v_0} U_{vk}^{v_0k*} U_{ck}^{v_0k}$. Writing the e - h interaction $-\sum_{vck,v'c'k'} V_{vck,v'c'k'} c_{c'k'}^\dagger c_{v'k'} c_{v'k'}^\dagger c_{ck} c_{ck}$ in the quasi-particle representation, we have

$$c_{c'k'}^\dagger c_{v'k'} = (U_{c'k'}^{n'k'*} \gamma_{n'k'}^\dagger) \times (U_{v'k'}^{m'k'} \gamma_{m'k'}), \quad c_{vk}^\dagger c_{ck} = (U_{vk}^{nk*} \gamma_{nk}^\dagger) \times (U_{ck}^{mk} \gamma_{mk}). \quad (S10)$$

With the above, H_{fluc} defined in Eq. S3 and Eq. S5 is equivalent to the fluctuation Hamiltonian in the maintext, and the derivation for the partition of the MF and fluctuation Hamiltonian is completed.

B. Order parameter fluctuations and optical properties

To evaluate fluctuations of the order parameter ($\delta\Delta_{vck}$) we define a perturbed ground state $|0'\rangle = |0\rangle + \alpha|S\rangle$, and $\delta\Delta_{vck}$ is expressed as

$$\begin{aligned}\delta\Delta_{vck} &= \lim_{\alpha \rightarrow 0} (\langle 0' | \sum_{v'c'k'} V_{v'c'k',vck} c_{v'k'}^\dagger c_{c'k'} | 0' \rangle - \Delta_{vck}) / \alpha \\ &= \langle 0 | \sum_{v'c'k'} V_{v'c'k',vck} c_{v'k'}^\dagger c_{c'k'} | S \rangle + \langle S | \sum_{v'c'k'} V_{v'c'k',vck} c_{v'k'}^\dagger c_{c'k'} | 0 \rangle,\end{aligned}\quad (\text{S11})$$

which is the Eq. 9 in the maintext. Transforming from c -operators to γ -operators, we write down the expression to be used in first-principles calculations,

$$\begin{aligned}\langle S | \sum_{v'c'k'} V_{v'c'k',vck} c_{v'k'}^\dagger c_{c'k'} | 0 \rangle &= \sum_{v'c'k'} V_{v'c'k',vck} \langle S | U_{v'k'}^{n'k'*} \gamma_{n'k'}^\dagger U_{c'k'}^{m'k'} \gamma_{m'k'} | 0 \rangle \\ &= \sum_{v'c'k'} V_{v'c'k',vck} U_{v'k'}^{n'k'*} U_{c'k'}^{m'k'} \langle S | \gamma_{n'k'}^\dagger \gamma_{m'k'} | 0 \rangle \\ &= \sum_{v''c'',v'c'k'} \left(V_{v'c'k',vck} U_{v'k'}^{c''k'*} U_{c'k'}^{v''k'} A_{v''c''k'}^S + V_{v'c'k',vck} U_{v'k'}^{v''k'*} U_{c'k'}^{c''k'} B_{v''c''k'}^S \right).\end{aligned}\quad (\text{S12})$$

$\langle 0 | \sum_{v'c'k'} V_{v'c'k',vck} c_{v'k'}^\dagger c_{c'k'} | S \rangle$ can be obtained similarly. Thus, the fluctuations of the order parameter can be readily calculated from first-principles.

For optical properties, the momentum operators are also transformed in the same manner,

$$P = \sum_{nmk} p_{nmk} c_{nk}^\dagger c_{mk} = \sum_{nmk} p'_{nmk} \gamma_{nk}^\dagger \gamma_{mk}, \quad p'_{nmk} = \sum_{n'm'} p_{n'm'k} U_{n'k}^{nk*} U_{m'k}^{mk}. \quad (\text{S13})$$

With Eq. 10 in the maintext, the optical conductivity is calculated using the Kubo formula,

$$\sigma_{\alpha\beta} = \frac{ine^2\delta_{\alpha\beta}}{(\omega + i\eta)m} + \frac{ie^2}{(\omega + i\eta)m^2} \sum_S \left(\frac{\langle 0 | P^\alpha | S \rangle \langle S | P^\beta | 0 \rangle}{\hbar\omega - \Omega_S + i\eta} - \frac{\langle 0 | P^\beta | S \rangle \langle S | P^\alpha | 0 \rangle}{\hbar\omega + \Omega_S + i\eta} \right). \quad (\text{S14})$$

C. 2-band form

In the limit of 2-band configuration, the U -matrix can be written as [53],

$$U = \begin{bmatrix} U_{ck}^{ck} & U_{ck}^{vk} \\ U_{vk}^{ck} & U_{vk}^{vk} \end{bmatrix} = \begin{bmatrix} u_k^* & v_k \\ -v_k^* & u_k \end{bmatrix}, \quad (\text{S15})$$

and the BSE kernel matrix is reduced to

$$\begin{aligned}\Pi_{kk'}^{AA} &= -V_{kk'} u_k^2 u_k^{*2} - V_{k'k} v_k^2 v_k^{*2} \\ \Pi_{kk'}^{AB} &= V_{kk'} v_k^{*2} u_k^{*2} + V_{k'k} u_k^{*2} v_k^{*2}.\end{aligned}\quad (\text{S16})$$

The interband momentum transition element $p'_{cvk} = (p_{cck} - p_{vvk})u_k v_k$ explains the brightness of collective modes of c_1 -type excitations in excitonic insulators in the maintext (p_{vck} is vanishing in the WSe₂-MoSe₂ bilayer due to the inserted vacuum of one layer hBN). For the c_2 -type, we have $\Pi_{kk'}^{AB} = 0$ as $v_k = U_{vc_2k} = 0$, which means TDA is good approximation. For the c_1 -type, we have finite $\Pi_{kk'}^{AB}$ as $v_k = U_{vc_1k}$ is nonvanishing which means that the c_1 -type excitations need the full BSE. Using the gauge in this 2-band U -matrix (Eq. S15), we find that phase mode fulfills $A_{vck}^P = -B_{vck}^P e^{i\theta_k}$ where $e^{i\theta_k}$ is the phase of the order parameter $\Delta_k = e^{i\theta_k} |\Delta_k|$.

D. Electron-electron and hole-hole interactions

In general, the total many-body Hamiltonian reads [56]

$$H_{tot} = \sum_{ck} \xi_{ck} c_{ck}^\dagger c_{ck} + \sum_{vk} \xi_{vk} c_{vk}^\dagger c_{vk} + \frac{1}{2} \sum_{\alpha\beta\alpha'\beta'} V_{\alpha\beta\alpha'\beta'} N(c_\alpha^\dagger c_\beta^\dagger c_{\beta'} c_{\alpha'}), \quad (\text{S17})$$

where N stands for normal-ordering with respect to the particle-hole representation of c -operators. The Hamiltonian in the Eq. 1 of maintext keeps only the e - h interaction in the two-body term. In principle, all other two-body terms can be treated in the same way as Eq. S10: first transform into quasiparticle representation by $c_{nk} = \sum_m U_{nk}^{mk} \gamma_{mk}$, then make them normal-ordered with respect to the γ -operator and it will end up with a one-body term and a two-body term in the quasiparticle representation. To illustrate, we use a configuration with only one valence and one conduction band (1V1C) as presented in the Section C of this Supplementary Material. Apart from the e - h interaction, we add the e - e and h - h direct interactions to the Hamiltonian,

$$H' = \sum_k \xi_{ck} c_{ck}^\dagger c_{ck} + \sum_k \xi_{vk} c_{vk}^\dagger c_{vk} - \sum_{kk'} V_{kk'}^{eh} c_{ck'}^\dagger c_{vk'} c_{vk}^\dagger c_{ck} + \sum_{kk'} V_{kk'}^{ee} c_{ck'}^\dagger c_{ck'} c_{ck}^\dagger c_{ck} + \sum_{kk'} V_{kk'}^{hh} c_{vk'}^\dagger c_{vk'} c_{vk}^\dagger c_{vk}. \quad (\text{S18})$$

The sign in front of each interaction denotes the nature of attraction/repulsion. The h_k and U -matrix in this 1V1C-configuration are written as

$$h_k = \begin{bmatrix} \xi_{ck} + \xi_{ck}^{ee} & -\Delta_k \\ -\Delta_k^* & \xi_{vk} - \xi_{vk}^{hh} \end{bmatrix}, \quad U = \begin{bmatrix} u_k^* & v_k \\ -v_k^* & u_k \end{bmatrix}, \quad (\text{S19})$$

where the extra one-body terms, ξ_{ck}^{ee} and ξ_{vk}^{hh} , in h_k come from the repulsive e - e and h - h interactions,

$$\begin{aligned} \sum_{kk'} V_{kk'}^{ee} c_{ck'}^\dagger c_{ck'} c_{ck}^\dagger c_{ck} &= \sum_{kk'} V_{kk'}^{ee} (|v_{k'}|^2 + c_{ck'}^\dagger c_{ck'} - |v_{k'}|^2) (|v_k|^2 + c_{ck}^\dagger c_{ck} - |v_k|^2) \\ &= H_0^{ee} + \sum_{kk'} (V_{kk'}^{ee} + V_{k'k}^{ee}) |v_{k'}|^2 c_{ck}^\dagger c_{ck} + H_{\text{fluc}}^{ee} \\ &= H_0^{ee} + \sum_{kk'} \xi_{ck}^{ee} c_{ck}^\dagger c_{ck} + H_{\text{fluc}}^{ee}. \end{aligned} \quad (\text{S20})$$

In the above equation, the two-body fluctuation term due to the e - e interaction reads

$$\begin{aligned} H_{\text{fluc}}^{ee} &= \sum_{kk'} u_{k'} v_{k'} u_k^* v_k^* (V_{kk'}^{ee} + V_{k'k}^{ee}) \gamma_{ck'}^\dagger \gamma_{vk'} \gamma_{vk}^\dagger \gamma_{ck} \\ &\quad + \sum_{kk'} u_{k'} v_{k'} u_k v_k V_{kk'}^{ee} \gamma_{ck'}^\dagger \gamma_{vk'} \gamma_{ck}^\dagger \gamma_{vk} + \sum_{kk'} u_k^* v_k^* u_k^* v_k^* V_{kk'}^{ee} \gamma_{vk'}^\dagger \gamma_{ck'} \gamma_{vk}^\dagger \gamma_{ck}. \end{aligned} \quad (\text{S21})$$

Similarly, we get ξ_{vk}^{hh} and H_{fluc}^{hh} . Thus, the extra one-body terms of ξ_{ck}^{ee} and ξ_{vk}^{hh} modify the MF calculation through h_k , while the extra two-body terms enter the BSE kernel,

$$\begin{aligned} \Pi_{kk'}^{AA} &= -V_{kk'} u_{k'}^2 u_k^{*2} - V_{k'k} v_{k'}^2 v_k^{*2} + u_{k'} v_{k'} u_k^* v_k^* (V_{kk'}^{ee} + V_{k'k}^{ee} + V_{kk'}^{hh} + V_{k'k}^{hh}) \\ \Pi_{kk'}^{AB} &= V_{kk'} v_{k'}^2 u_k^{*2} + V_{k'k} u_{k'}^2 v_k^{*2} + u_{k'}^* v_{k'}^* u_k^* v_k^* (V_{kk'}^{ee} + V_{k'k}^{ee} + V_{kk'}^{hh} + V_{k'k}^{hh}). \end{aligned} \quad (\text{S22})$$

Therefore, one could calculate all the many-body effects from first-principles as discussed in the maintext. For the numerical demonstration of WSe₂-MoSe₂ bilayer structure, the repulsive effect from e - e and h - h interactions can be compensated by the bias chemical potential μ . And the intrinsic interband tunneling effect from the two-body term in Eq. S17, containing one conduction (valence) and three valence (conduction) bands, can be neglected as the wave function overlap between the two layers is vanishing due to the inserted vacuum of one layer hBN. So we take the simple Hamiltonian with only e - h interactions in the numerics of maintext. For bulk excitonic insulator materials, other many-body interactions can be important for accurate *ab initio* calculations.

E. Dielectric screening from exciton condensate

In this section, we discuss the extra screening effect in the presence of exciton condensation. The major effect of the e - h interaction in Eq. S2 is the direct term that depends on the screened Coulomb potential $W(r, r', \omega)$. In reciprocal space, the screened Coulomb potential is determined by the dielectric matrix [64, 65],

$$W_{GG'}(q, \omega) = \frac{1}{(2\pi)^6} \int e^{-i(q+G)r} W(r, r', \omega) e^{i(q+G')r'} dr dr' = \epsilon_{GG'}^{-1}(q, \omega) v_{q+G}, \quad (\text{S23})$$

where $v_{q+G} = 4\pi/|q+G|^2$ is the Coulomb potential. Using the Random Phase Approximation, the dielectric matrix is calculated from the non-interacting polarizability matrix [51]

$$\epsilon_{GG'}(q, \omega) = \delta_{GG'} - v_{q+G} \chi_{GG'}(q, \omega), \quad (\text{S24})$$

We note that in principle one should calculate frequency-dependent dielectric function, which means that the gap equation and BSE should be solved self-consistently with updated $\epsilon_{GG'}(q, \omega)$. In the numerical demonstration, we neglect the dynamical screening effect[74] and the static polarizability matrix is calculated by [65],

$$\chi_{GG'}(q, 0) = \chi_{GG'}(q) = \frac{2}{\Omega} \sum_{vck} \frac{\langle \psi_{vk} | e^{-i(q+G)r} | \psi_{ck+q} \rangle \langle \psi_{ck+q} | e^{i(q+G')r'} | \psi_{vk} \rangle}{E_{vk} - E_{ck+q}}. \quad (\text{S25})$$

For the normal Kohn-Sham state in WSe₂-MoSe₂, the wave function overlap between the two layers can be neglected and the total polarizability is the sum of the individual layer [60]. As the excitonic order parameter is developed, the top valence and top conduction band on the two layers starts to mix into the quasiparticle wave function $\psi_{mk}^B = \sum_n U_{nk}^{mk*} \psi_{nk}$. Therefore, after obtaining the EI state, we need to calculate the extra dielectric screening from the exciton condensate. Here, due to limitation of computational resource, we approximate $\chi_{GG'}(q) \approx \chi_{GG'}^{\text{BL}}(q) + \chi_{GG'}^{\text{EI}}(q)$, where $\chi_{GG'}^{\text{BL}}(q)$ is the original polarizability of the bilayer and $\chi_{GG'}^{\text{EI}}(q)$ is evaluated using only the quasiparticle transition at K with an effective number of condensate region k -points on the $210 \times 210 \times 1$ k -grid,

$$\chi_{GG'}^{\text{EI}}(q) = \frac{2}{\Omega} \bar{N}_K \frac{\langle \psi_{vK}^B | e^{-i(q+G)r} | \psi_{cK+q}^B \rangle \langle \psi_{cK+q}^B | e^{i(q+G')r'} | \psi_{vK}^B \rangle}{E_{vK} - E_{cK+q}}, \quad (\text{S26})$$

where $\bar{N}_K = \sum_k |U_{vc1k}|^2 / |U_{vc1K}|^2$. As the exciton density in the BCS regime is much larger than the BEC regime, we update the dielectric screening from χ^{EI} for the BCS regime as stated in the maintext. We note that a convergent dielectric screening from the condensed excitons with better calculation accuracy can be potentially important in the BCS regime.

F. Computational details

The density functional theory (DFT) and many-body perturbation theory (MBPT) calculations in this work are performed within the QuantumESPRESSO [49, 50] and BerkeleyGW [51] packages. Optimized norm-conserving Vanderbilt pseudopotentials [67] with a kinetic energy cut-off of 60 Ry and Perdew-Becke-Ernzerhof approximation of the exchange correlation functional [69] are used. The Brillouin zone (BZ) sampling k -grid for the DFT self-consistent calculation is $36 \times 36 \times 1$. The GW band gap without bias voltage is calculated using $12 \times 12 \times 1$ q/k -grid and 8 Ry G -vector cutoff. The DFT wave functions on the BZ-patch with radius of 0.21 \AA^{-1} from K/K' on a dense k -grid of $210 \times 210 \times 1$ are prepared for the calculation of $e\text{-}h$ interaction kernel $V_{vck, v'c'k'}$. In the Eq. 1 of the maintext, $\xi_{ck} = \epsilon_{ck} + \mu$ where ϵ_{nk} is the Kohn-Sham energies and the bias voltage μ is treated by scissor-operation. A fine q -grid is generated by $q = k - k'$ where k/k' is on the dense k -grid BZ-patch. The dielectric matrix on this q -grid is calculated using $6 \times 6 \times 1$ k -grid sampling, 8 Ry G -vector cutoff and 500 empty bands. The slab coulomb truncation [71] is adopted and no symmetry is used to reduce the k -grid throughout the calculation of dielectric function and the $e\text{-}h$ interaction kernel. After we get ξ_{ck} and $V_{vck, v'c'k'}$ from standard DFT and MBPT calculations using QuantumESPRESSO and BerkeleyGW, the MF calculation for EI ground state includes diagonalization of h_k and calculation of Δ_{vck} using Eq. S9 self-consistently. Then we construct the BSE and solve it numerically for the many-body excitation energies and excited states. The fluctuation of order parameter for each collective mode is calculated using Eq. 9 in the maintext. We also performed calculation for the 1V1C-configuration without spin-orbital-coupling (SOC) including both K and K' valley (see Fig. S4). K and K' valley are degenerate so that we focus on K valley for the 1V2C-configuration in the maintext. Band convergence result in Fig. S5 further shows that higher energy conduction bands do not affect the excitation spectrum in the EI state.

II. SUPPLEMENTARY FIGURES

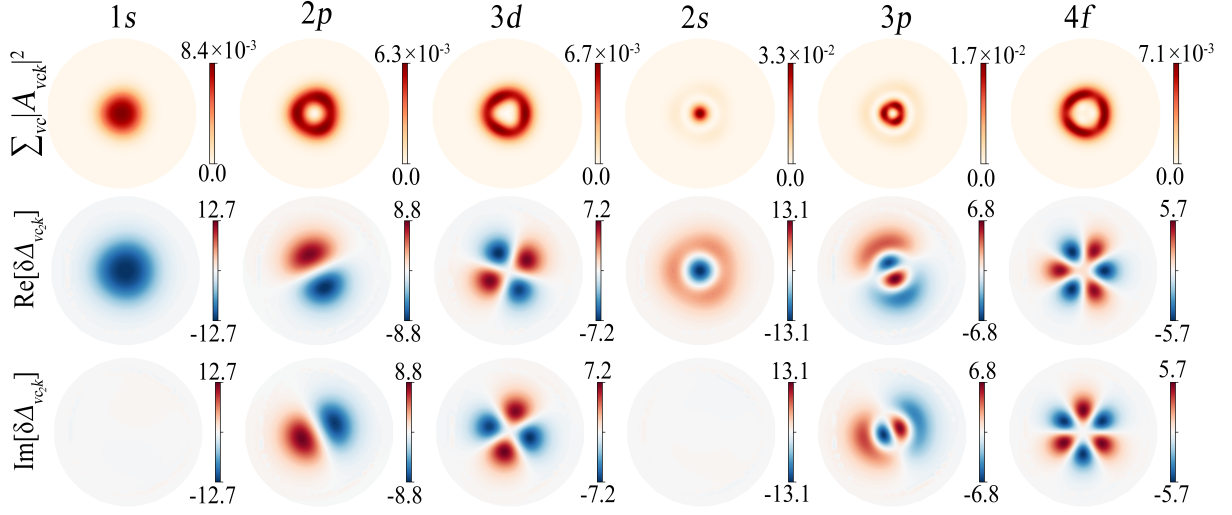


FIG. S1. Plot of $\sum_{vc} |A_{vc,k}|^2$ and the real and imaginary parts of $\delta\Delta_{vc_2,k}$ (meV) for a few c_2 -type collective excitations on the momentum plane corresponding to the blue labels in Fig. 2(b) of the maintext.

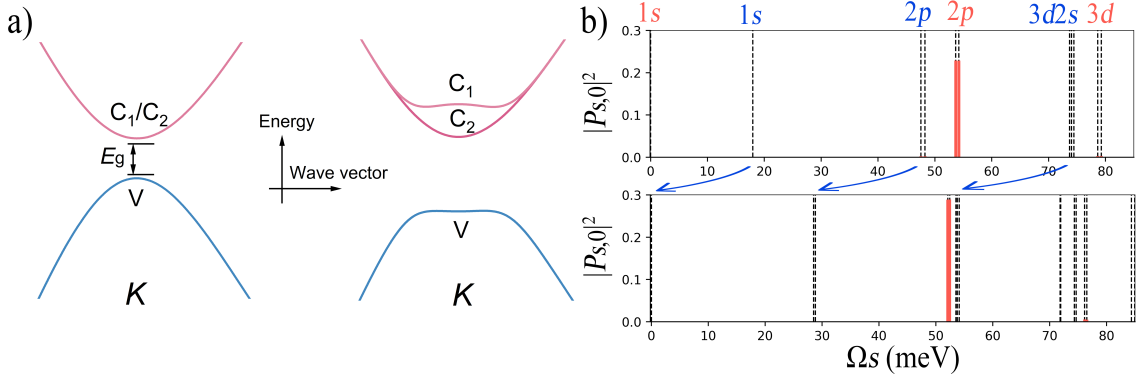


FIG. S2. (a) Band structure of normal state and EI state for 1V2C-configuration with artificially degenerate conduction bands. (b) Excitation spectrum for 1V2C-configuration with calculated SOC-splitting (upper) and artificially degenerate (lower) conduction bands. Red and blue labels on top refers to c_1 - and c_2 -type excitations, respectively. The c_2 -type excitations are redshift by the SOC splitting indicated by the blue arrows. The 1s c_2 -type excitation becomes another gapless mode in the limit of zero SOC splitting as discussed in the maintext.

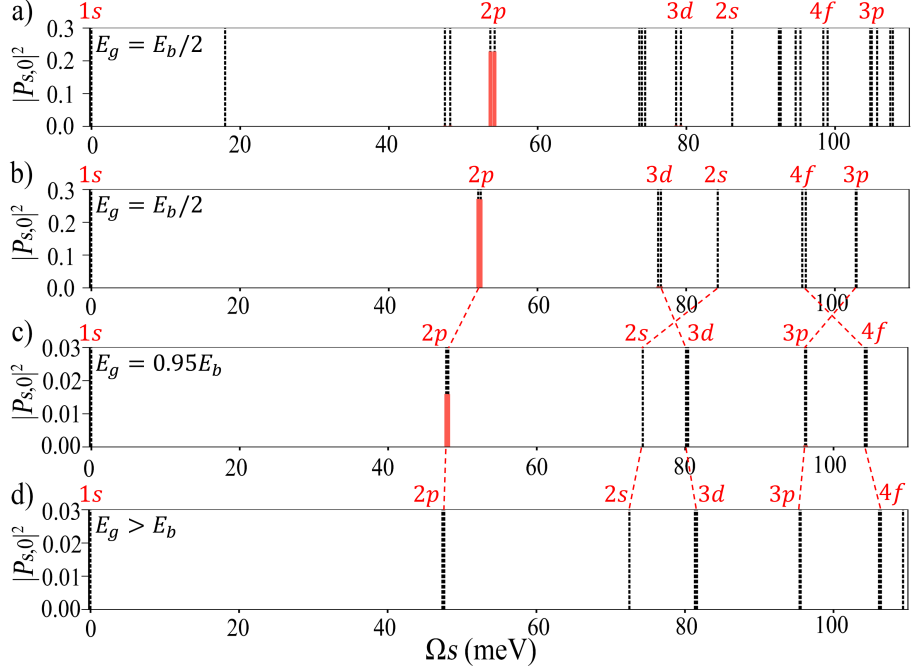


FIG. S3. The excitation spectrum labeled by corresponding quantum numbers calculated from the BSE. (a) 1V2C-configuration results reproduced from Fig. 2(b) in the maintext. Only c_2 -type excitations are labeled. (b-d) 1V1C-configuration results with different E_g . For $E_g > E_b$, the excitation energies Ω_S are subtracted by the $1s$ -state energy. (b-d) are computed without SOC effect.

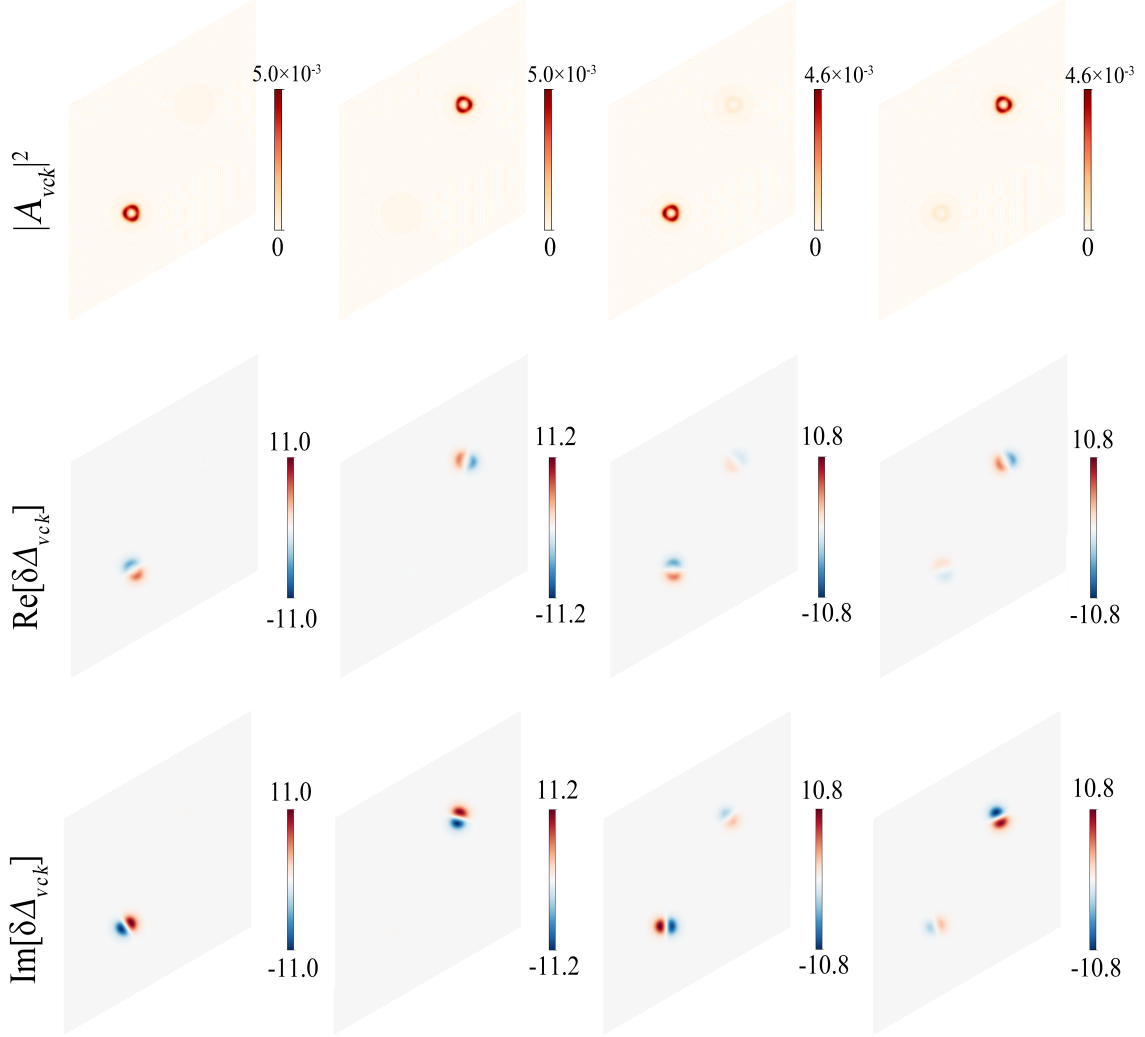


FIG. S4. Plot of $|A_{vck}|^2$ and the real and imaginary parts of $\delta\Delta_{vck}$ (meV) for all $2p$ modes of $1V1C$ -configuration including both K and K' valleys.

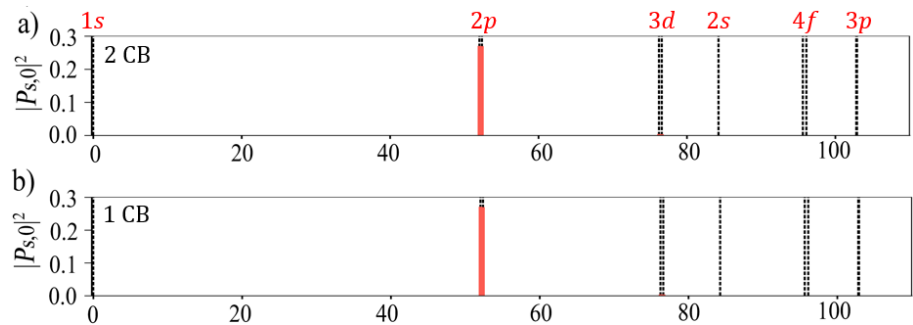


FIG. S5. Band convergence for the BSE calculated excitation spectrum with 2 (a) and 1 (b) conduction bands using the system without SOC effect. (b) is the same as Fig.S3(b).